Interplay between Rab35 and Arf6 controls cargo recycling to coordinate cell adhesion and migration

Patrick D. Allaire*, Mohamed Seyed Sadr*, Mathilde Chaineau, Emad Seyed Sadr, Sarah Konefal, Maryam Fotouhi, Deborah Maret, Brigitte Ritter, Rolando F. Del Maestro and Peter S. McPherson‡

Department of Neurology and Neurosurgery, Montreal Neurological Institute, McGill University, Montreal, QC H3A 2B4, Canada

*These authors contributed equally to this work
‡Author for correspondence (peter.mcpherson@mcgill.ca)

Accepted 19 November 2012
Journal of Cell Science 126, 722–731
© 2013. Published by The Company of Biologists Ltd
doi: 10.1242/jcs.112375

Summary

Cells inversely adjust the plasma membrane levels of integrins and cadherins during cell migration and cell–cell adhesion but the regulatory mechanisms that coordinate these trafficking events remain unknown. Here, we demonstrate that the small GTPase Rab35 maintains cadherins at the cell surface to promote cell–cell adhesion. Simultaneously, Rab35 supresses the activity of the GTPase Arf6 to downregulate an Arf6-dependent recycling pathway for β1-integrin and EGF receptors, resulting in inhibition of cell migration and attenuation of signaling downstream of these receptors. Importantly, the phenotypes of decreased cell adhesion and increased cell migration observed following Rab35 knock down are consistent with the epithelial–mesenchymal transition, a feature of invasive cancer cells, and we show that Rab35 expression is suppressed in a subset of cancers characterized by Arf6 hyperactivity. Our data thus identify a key molecular mechanism that efficiently coordinates the inverse intracellular sorting and cell surface levels of cadherin and integrin receptors for cell migration and differentiation.

Key words: ACAP2, Cadherin, Cancer, EGF receptor, Epithelial–mesenchymal transition, EMT, Erk, Glioma, Integrin, Tumor invasiveness

Introduction

The migratory potential of cells is determined by the composition of the receptor proteome present at the cell surface. Integrins engage components of the extracellular matrix and enhanced internalization and recycling of integrins is essential for cell migration (reviewed in Margadant et al., 2011). On the other hand, surface-expressed cadherins form homophilic interactions that promote cell–cell contact and therefore inhibit cell migration (Huttenlocher et al., 1998; Delva and Kowalczyk, 2009). It is thus imperative for cells to balance the surface levels of these receptors in order to go through complex cellular programs such as cell migration during development and cell–cell adhesion during tissue differentiation.

The cell surface proteome is in constant flux, new molecules are added from the secretory pathway and through translocation from endosomal compartments, while endocytosis removes receptors and other proteins from the surface and delivers them to endosomes. At the level of endosomes, receptors are sorted for retention, recycling or lysosomal degradation and thus, factors controlling endosomal sorting decisions strongly influence the protein composition of the plasma membrane and resulting cell functions (Maxfield and McGraw, 2004; Hsu and Prekeris, 2010). The Arf and Rab families of small GTPases, which switch between inactive GDP-bound conformations and active GTP-bound conformations, are critical regulators of membrane trafficking (reviewed in Kawasaki et al., 2005). Once activated by guanine nucleotide exchange factors (GEFs), GTP-bound Arfs and Rabs recruit a plethora of effectors that have many functions including the formation of cargo carriers on multiple organelles including endosomes, the recruitment of appropriate cargo into those carriers, and the routing of the carriers to the appropriate site of fusion. With the help of GTPase activating proteins (GAPs), the GTPases hydrolyse the GTP to GDP, thus terminating the process.

Arf6 is a well-studied member of the Arf family and functions in the endocytosis of a wide variety of receptor molecules including integrins and cadherins (Schweitzer et al., 2011). In addition, Arf6 activity is required for endosomal sorting of cargo, with different cargo having different fates. For example, active Arf6 prevents the recycling of E-cadherin, leading to intracellular retention or degradation with disruption of cell–cell contacts (Palacios et al., 2001; Palacios et al., 2002; Frasa et al., 2010). Consistently, downregulation of Arf6 activity by EphA2 and Robo4 signaling enhances E- and VE-cadherin-mediated cell–cell contacts (Miura et al., 2009; Jones et al., 2009). On the other hand, Arf6 activity increases the recycling of integrins, causing upregulation of integrin levels and signaling, leading to the formation of actin-based membrane protrusions associated with migration and invasion including lamellipodia (Santy and Cassanova, 2001), membrane ruffles (Zhang et al., 1999; Radhakrishna, 1999), podosomes (Svensson et al., 2008), and invadopodia (Hashimoto et al., 2004; Tague et al., 2004). The Arf6-driven loss of cell–cell adhesion, increased motility and changes in cell morphology are all facets of a process referred to as the epithelial–mesenchymal transition (EMT) (Thiery, 2003). EMT is a feature of embryogenesis that is vital for morphogenesis during development (Kong et al., 2010) and it shares many phenotypic similarities with invasive cancer cells (Polyak and Weinberg, 2009; Micalizzi et al., 2010). Consistently, Arf6 activity is upregulated in several epithelial

and non-epithelial cancers such as breast, lung and brain cancer (Li et al., 2006; Morishige et al., 2008; Sabe et al., 2009; Li et al., 2009; Hu et al., 2009; Menju et al., 2011).

A second small GTPase necessary for efficient recycling of cargo from endosomes is Rab35. Once activated by its specific GEFs, the connecdenn/DENND1 family of proteins (Allaire et al., 2010; Marat and McPherson, 2010), Rab35 drives the recycling of a wide variety of cargo including MHC class I (Allaire et al., 2010) and MHC class II (Walseng et al., 2008), T-cell receptor (Patino-Lopez et al., 2008), the calcium activated potassium channel $KCa^{2+}2.3$ (Gao et al., 2010), exosomes (Hsu et al., 2010) and synaptic vesicles (Uytterhoeven et al., 2011). Rab35 also functions during cell division to recycle lipid and protein components necessary for furrow ingression (Kouranti et al., 2006; Dambournet et al., 2011). Interestingly, recent studies have demonstrated an intimate relationship between Rab35 and Arf6. Specifically, Arf6 binds the Rab35 GAPs TBC1D10A (Hanono et al., 2006), TBC1D10B (Chesneau et al., 2012) and TBC1D24/Skywalker (Uytterhoeven et al., 2011), and expression of constitutively active Arf6 leads to defects in cytokineses and the accumulation of binucleated cells due to Arf6-mediated inhibition of Rab35 (Chesneau et al., 2012). Based on these observations, Arf6 has been placed upstream of Rab35. By contrast, Rab35 binds to the Arf6 GAP ACAP2/centaurinβ recruiting ACAP2 to Arf6-positive endosomes (Kanno et al., 2010; Rahajeng et al., 2012; Kobayashi and Fukuda, 2012), which places Rab35 upstream of Arf6.

We now demonstrate that Rab35 and Arf6, through mutual antagonism, are geared to reciprocally balance the recycling of integrins and cadherins in order to tune cell adhesive behavior towards cell migration or intercellular contact. In particular, we find that Rab35 activity is essential to maintain cadherins at the cell surface to promote cell–cell adhesion, suggesting that the well-established antagonistic effect of active Arf6 on cadherin recycling is mediated through inhibition of Rab35. We also find that Rab35 negatively regulates integrin recycling and cell migration through its inhibition of Arf6, driven by ACAP2 recruitment to active Rab35. Consistently, Rab35 knock down leads to enhanced Arf6 activity, recycling of integrins as well as EGF receptor, which is known to co-traffic with integrins, and increased cell migration. Importantly, given that Arf6 activity levels are upregulated in numerous tumors (Li et al., 2006; Morishige et al., 2008; Sabe et al., 2009; Li et al., 2009; Hu et al., 2009; Menju et al., 2011), we find that Rab35 levels are downregulated in surgically resected human tumors known for Arf6 hyperactivity including gliomas. Together, our data reveal that the functional interplay between Rab35 and Arf6 provides the molecular underpinnings for efficient coordination of cell migration and cell–cell adhesion.

Results

Rab35 is required to maintain cadherin surface levels and cell–cell adhesion

We previously demonstrated that Rab35 and its GEF, connecdenn 1/DENND1A are required for the endosomal recycling of MHC class I since knock down of either protein causes retention of internalized MHC class I in an endosomal-recycling compartment (Allaire et al., 2010). We sought to identify additional cell surface receptors that require Rab35 for recycling. We used previously established shRNAmiR sequences to knock down Rab35 (Allaire et al., 2010) (Fig. 1A). Upon Rab35 knock down in COS-7 cells, endogenous N-cadherins lose their cell surface localization and accumulate in an intracellular compartment together with MHC class I (Fig. 1B). Similar results are seen with E-cadherin transfected into COS-7 cells (supplementary material Fig. S1). Moreover, surface biotinylation assays reveal significantly reduced levels of endogenous cadherin at the surface of Rab35 knock down cells (Fig. 1C,D). To determine if Rab35 is required for cell–cell adhesion, we performed cell aggregation assays. Suppression of Rab35 expression efficiently prevents dissociated cells from aggregating after 20 minutes (Fig. 1E,F) and even after 60 minutes, a significant number of cells deprived of Rab35 remain single (Fig. 1F). Similar results are observed in U251 cells, a line derived from a human glioblastoma (supplementary material Fig. S2A). Thus, Rab35 is necessary to maintain cadherins at the cell surface, perhaps by allowing for efficient recycling, and Rab35 is also required for the ability of cells to form cell–cell contacts.

Rab35 suppresses β1-integrin recycling and cell motility

Downregulation of adhesive cell surface cadherin is a hallmark of cancer progression and is associated with changes in cell morphology and enhanced cellular motility (Huttenlocher et al., 1998; Jakob et al., 1998; Blindt et al., 2004; Shoval et al., 2007; Maret et al., 2010). To determine if Rab35 knock down leads to an increase in cell motility we used a scratch assay, demonstrating that Rab35 loss of function significantly stimulates cell migration in both COS-7 (Fig. 2A,B) and U251 cells (supplementary material Fig. S2B). Re-expression of an shRNAmiR-resistant (mouse) Rab35 construct rescues the cell migration phenoype (Fig. 2C) demonstrating that the phenotype is due to loss of Rab35 function. Since cell migration depends on β1-integrin recycling (Gu et al., 2011), we labeled the internal pool of β1-integrin by incubating cells with an antibody recognizing the extracellular domain followed by stripping of residual surface antibody, and determined the amount of resurfacing antibody over time. Rab35 knock down significantly increases β1-integrin recycling (Fig. 2D) and consistently, FACS analysis shows an increase in the surface pool of β1-integrin in Rab35 knock down cells (Fig. 2E). In fact, western blot analysis of crude cell lysates reveals an overall increase in β1-integrin levels (Fig. 2F,G), suggesting that in the absence of Rab35, enhanced recycling reroutes β1-integrin away from lysosomal degradation towards the cell surface.

In addition to enhanced β1-integrin recycling, cell migration also depends on β1-integrin activation and signaling to focal adhesion kinase (FAK) (Lipfert et al., 1992). In Rab35 knock down cells the levels of FAK tyrosine phosphorylation, used as a measure of activity are significantly upregulated while total levels of FAK remain unchanged (Fig. 2F,G). Together, these data reveal that Rab35 knock down cells adapt to the requirements for enhanced motility by shifting cadherins away from the cell surface to decrease cell–cell adhesion, while upregulating β1-integrin recycling and signaling.

Rab35 controls cell migration through negative regulation of Arf6

It is established that activation of Arf6 enhances β1-integrin recycling and signaling and β1-integrin-mediated cell migration (Arjonen et al., 2012). Given that the Arf6 GAP ACAP2 is a Rab35 effector that is recruited to Arf6-positive endosomes by

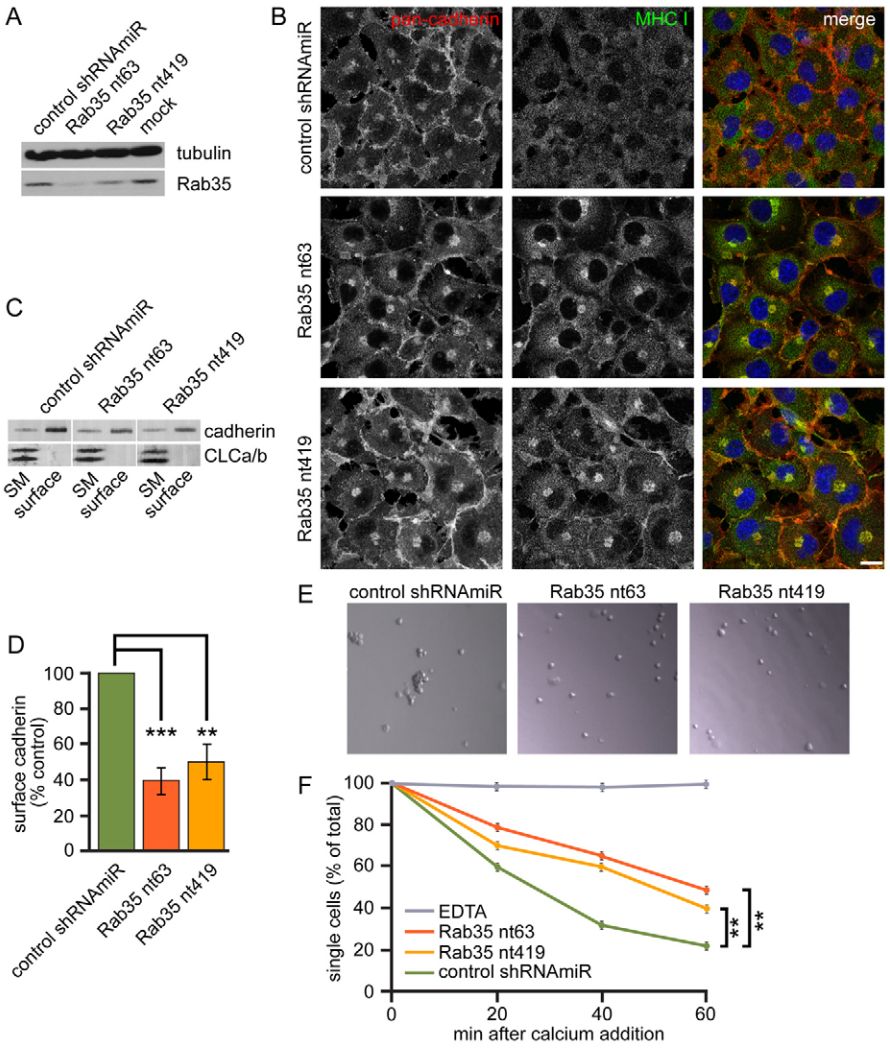

Fig. 1. Rab35 knock down inhibits cadherin recycling and intercellular adhesion. For all panels, COS-7 cells were treated with control shRNAmiR or two different shRNAmiRs targeting Rab35 (Rab35 nt63 and Rab35 nt419) as indicated. (**A**) Cells were processed for western blot with antibodies recognizing Rab35 or tubulin. (**B**) Cells were stained for endogenous cadherin using a rabbit polyclonal pan-cadherin antibody (COS-7 cells express N-cadherin) and a mouse monoclonal antibody recognizing endogenous MHC class I. Scale bar: 10 μm. (**C**) Cells were biotinylated at 4°C and detergent-solubilized cell lysates prepared. The biotinylated cell surface proteins were precipitated using streptavidin-agarose beads. Proteins bound to the beads were processed for western blot with a pan-cadherin antibody or an antibody that recognizes clathrin-light chains a and b (CLCa/b). An aliquot of the cell lysate (starting material, SM) equal to 10% of that added to the beads was processed in parallel. (**D**) Quantification of the percentage of total cadherin at the cell surface determined as in C. Error bars represent s.d. and statistical analysis employed a repeated-measure one-way ANOVA followed by a Dunnett's post-test on six experiments. (**E**) Cells were treated with 2 mM EDTA to dissociate monolayers into single cells. The cells were then pelleted, washed and resuspended in Ca^{2+}-containing culture media. Cells were agitated gently and 50 μl aliquots of cell suspension were analyzed at 20-minute intervals. (**F**) Quantification of three duplicate aggregation assays as shown in E. For each time point, ~200 cells were analyzed. Error bars represent s.e.m. and statistical analysis employed a repeated-measure two-way ANOVA followed by a Bonferroni post-test. $^{**}P<0.01$, $^{***}P<0.001$.

Rab35 (Kanno et al., 2010; Kobayashi and Fukuda, 2012), it is probable that Rab35 knock down stimulates β1-integrin activity by relieving a physiological suppression of Arf6. To address this, we analyzed the levels of active Arf6 in control and Rab35 knock down cells in effector binding assays using the Arf6 effector GGA3. ACAP2 binds exclusively to the constitutively active Rab35 variant Q67L (Fig. 3A), consistent with previous studies (Kanno et al., 2010; Rahajeng et al., 2012; Kobayashi and Fukuda, 2012), and we demonstrate here that Rab35 knock down significantly enhances endogenous Arf6 activity (Fig. 3B,C), showing directly that Rab35 is a negative regulator of Arf6.

Since Arf6 activation is required for β1-integrin recycling, we tested whether the increase in cell migration observed with Rab35 depletion results from stimulation of the Arf6 recycling pathway. Interestingly, the enhanced cell migration resulting from Rab35 knock down is reversed by simultaneous knock down of Arf6 (Fig. 3D,E), supporting the concept that Rab35 supresses Arf6 to limit cell migration. To address whether the intracellular accumulation of cadherin and decrease in cell–cell adhesion seen following Rab35 knock down (Fig. 1) is also a reflection of enhanced activity of Arf6, we tested double knock down cells in aggregation assays. Importantly, Arf6 knock down does not reverse the decrease in cell–cell adhesion resulting from Rab35 knock down (Fig. 3F). Thus, Rab35 directly promotes activities that maintain cadherin on the cell surface while simultaneously inhibiting Arf6 to suppress β1-integrin recycling (Fig. 3G), identifying Rab35 as a crucial regulator of intracellular receptor sorting that inversely coordinates cell–cell adhesion and cell migration.

Rab35 suppresses EGF receptor signaling and cell proliferation

EGF receptor co-traffics with β1-integrin (Muller et al., 2009) and we thus sought to evaluate EGF receptor recycling following Rab35 knock down. We labeled the internal pool of the receptor by incubating cells with an antibody against the extracellular domain followed by stripping of residual cell surface antibody, and measured the amount of resurfacing antibody over time. As for β1-integrin (Fig. 2D), the recycling of EGF receptor is significantly increased in Rab35 knock down cells (Fig. 4A). In addition, FACS analysis confirms that the surface pool of EGF receptor is increased (Fig. 4B) while western blot analysis of cell lysates reveals an increase in the overall levels of the receptor (Fig. 4C,D). Together, these data suggest that enhanced recycling reroutes EGF receptor away from lysosomal degradation, allowing for receptor accumulation at the cell surface.

Journal of Cell Science

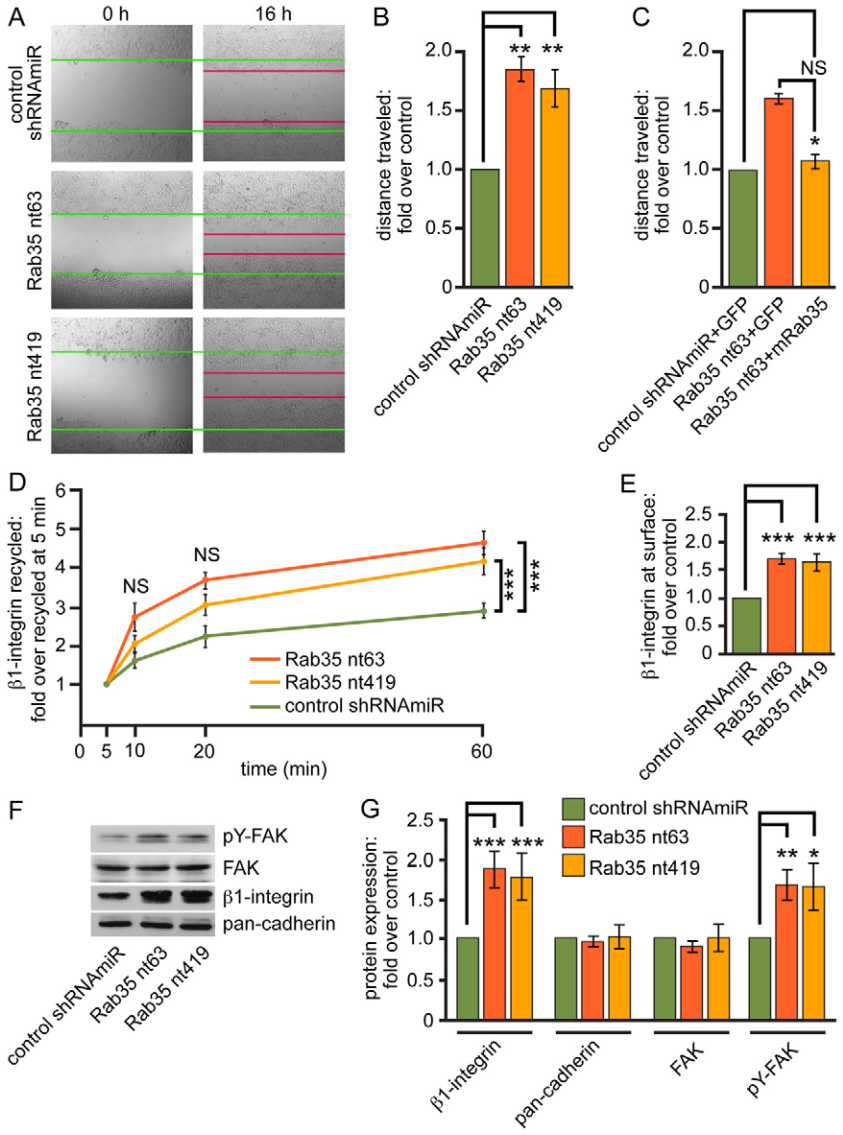

Fig. 2. Rab35 knock down enhances pro-migratory signaling. For all panels, COS-7 cells were treated with control shRNAmiR or two different shRNAmiRs targeting Rab35 (Rab35 nt63 and Rab35 nt419) as indicated. (**A**) A scratch was made in a confluent monolayer of cells and images were obtained immediately after the scratch (0 hours) and after 16 hours. Green and red lines mark the front of migration at 0 and 16 hours, respectively. (**B**) Quantification of cell migration of four replicate experiments as in A. Error bars represent s.e.m. and statistical analysis employed a repeated-measure one-way ANOVA followed by a Dunnett's post-test. (**C**) Rab35 knock down cells were transduced with a lentivirus driving the formation of mouse Rab35, which is resistant to the human shRNAmiR, and three replicate cell migration experiments were quantified. Error bars represent s.e.m. and statistical analysis employed a repeated-measure one-way ANOVA followed by a Dunnett's post-test. (**D**) β1-integrin recycling at the indicated time points determined by FACS-based analysis of the resurfacing of a previously internalized β1-integrin antibody. Data represent four duplicate experiments. Error bars indicate s.d. and statistical analysis employed a repeated-measure two-way ANOVA followed by a Bonferroni post-test. (**E**) β1-integrin surface levels determined by FACS-based analysis of cells incubated at 4℃ with an antibody against β1-integrin. The graph shows the average fold increase in knock down cells relative to control in four experiments. Error bars represent s.d. and statistical analysis employed a repeated-measure one-way ANOVA followed by a Dunnett's post-test. (**F**) Total cell lysates were processed for western blot with an antibody that specifically recognizes FAK phosphorylated at Tyr738 (pY-FAK) or with antibodies recognizing FAK, β1-integrin or cadherin, as indicated. (**G**) Quantification of results shown in F. The graph shows the average fold increase in knock down cells relative to control in four experiments. Error bars represent s.d. and statistical analysis employed a repeated-measure one-way ANOVA followed by a Dunnett's post-test. $*P<0.05$, $**P<0.01$, $***P<0.001$; NS, not significant.

EGF receptor signals from both the cell surface and endosomes and receptor signaling required for cell migration and proliferation is thought to occur primarily in recycling/signaling endosomes (Lenferink et al., 1998; Worthylake et al., 1999; Caswell et al., 2008; Muller et al., 2009). Under normal conditions, EGF receptors are sorted to lysosomes terminating signaling while in Rab35 knock down cells, the receptors appear to be rerouted to the recycling pathway. β1-integrin receptors also appear to be re-routed to the recycling pathway and consistently, internalized EGF and β1-integrin receptors co-distribute in enlarged intracellular vesicles in Rab35 knock down cells (supplementary material Fig. S3). EGF receptor partitioning into the recycling pathway following Rab35 knock down should increase EGF-stimulated signaling cascades. We thus examined EGF receptor activity by blotting cell lysates for receptor phosphorylation at Y1068 and Y1148, docking sites for Grb2 and Shc that when occupied lead to activation of Erk1/2 and Akt (Rojas et al., 1996; Zwick et al., 1999; Rodrigues et al., 2000; Mattoon et al., 2004). Phosphorylation at both sites is increased proportionally to the increase in total EGF receptor following Rab35 knock down (Fig. 4C,D), indicating that while there is a constant fraction of the receptor pool being phosphorylated, Rab35 knock down yields a net increase in the total amount of activated receptor. In addition, we detected enhanced activation of both Erk1/2 and Akt (Fig. 4D,E). Given the enhanced activity of the pro-mitotic EGF receptor/Erk/Akt pathway, we tested for changes in cell proliferation. Knock down of Rab35 significantly increases proliferation rates, with doubling times reduced by close to 3 hours from 26.2 to 23.6 hours (Fig. 4E). Similarly, knock down of Rab35 in U251 cells decreases the doubling time by ~4.5 hours (supplementary material Fig. S2C). Thus, Rab35 controls cell growth, likely by regulating EGF receptor expression and activity.

Rab35 expression is decreased in malignant tumors

In all, Rab35 knock down causes reduced cell–cell adhesion, enhanced recycling and signaling of β1-integrin and EGF receptors, increased cell migration and pro-mitotic signaling. This is reminiscent of an EMT, which is accompanied by a characteristic change in cell morphology that includes an

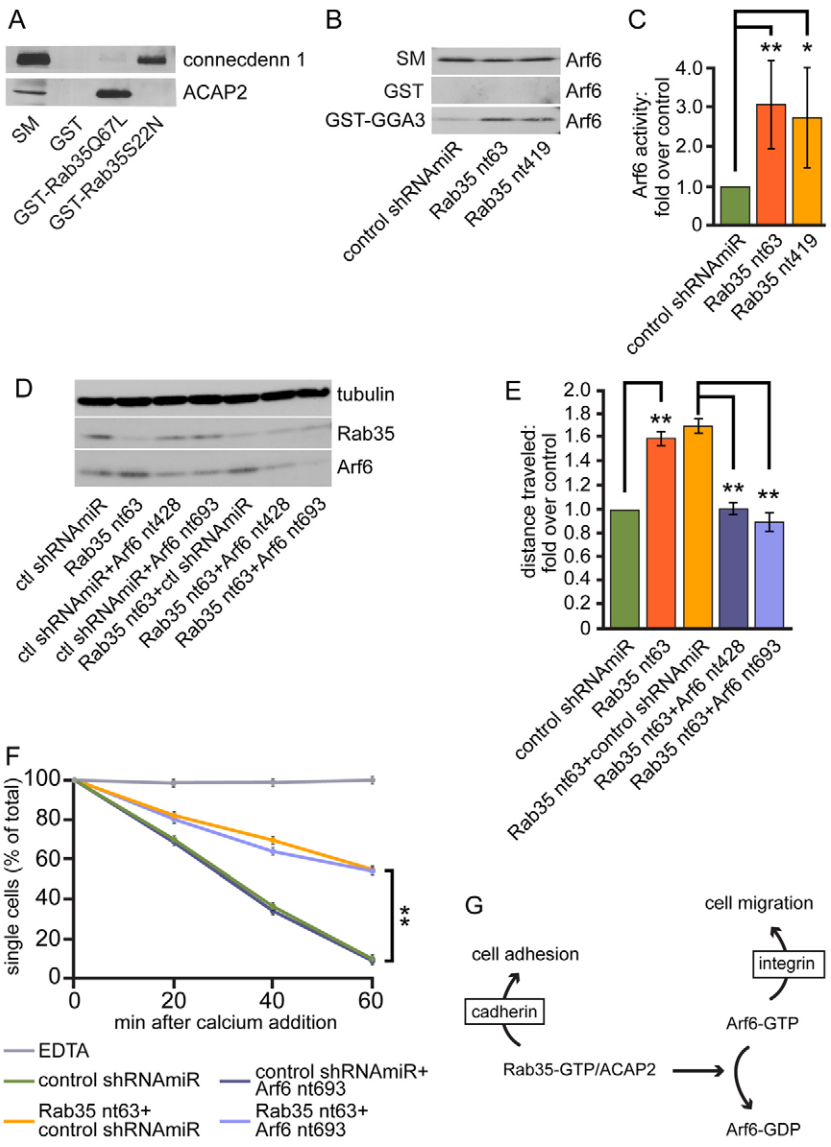

Fig. 3. Rab35 directly regulates cadherin recycling and inhibits Arf6 activity required for cell migration. (**A**) GST-GTP-locked Rab35 (GST-Rab35Q67L), GST-GDP-locked Rab35 (GST-Rab35S22N) and GST alone coupled to glutathione-Sepharose were incubated with lysates from HEK-293 cells expressing FLAG-ACAP2. Proteins specifically bound to the beads were prepared for western blot with anti-FLAG antibody (ACAP2) or with antibody recognizing endogenous connecdenn 1, which specifically binds Rab35-GDP. (**B**) GST-GGA3 or GST alone, coupled to glutathione-Sepharose were incubated with lysates from Rab35 knock down cells (Rab35 nt63 and Rab35 nt419) or control cells. Proteins specifically bound to the beads were processed for western blot with an antibody recognizing endogenous Arf6. An aliquot of starting material (SM) equal to 10% of the lysate added to the beads was processed in parallel. (**C**) Quantification of five independent experiments performed as in B. Error bars represent s.d. Statistical analysis employed a repeated-measure one-way ANOVA followed by a Dunnett's post-test. (**D**) COS-7 cells were treated with control shRNAmiR, shRNAmiR targeting Rab35 (Rab35 nt63), control shRNAmiR in combination with shRNAmiRs targeting Arf6 (Arf6 nt428 and Arf6 nt693) and shRNAmiR targeting Rab35 in combination with shRNAmiRs targeting Arf6. Lysates from the cells were processed for western blot with antibodies recognizing tubulin, Rab35 and Arf6. (**E**) Quantification of cell migration assays performed as in Fig. 2 on cells treated with control shRNAmiR or shRNAmiRs targeting Rab35, Arf6 or combinations of both, as indicated. Four duplicate experiments were analyzed. Error bars represent s.e.m. Statistical analysis employed a repeated-measure one-way ANOVA followed by a Dunnet's post-test. (**F**) Quantification of three replicate aggregation assays performed as in Fig. 1 on cells treated with control shRNAmiR or shRNAmiRs targeting Rab35, Arf6 or combinations of both, as indicated. Error bars represent s.e.m. and statistical analysis employed a repeated-measure two-way ANOVA followed by a Bonferroni post-test. (**G**) Model of the role of Rab35 in regulating cell adhesion. Rab35-GTP activates cadherin recycling upregulating cell adhesion while downregulating the activity of Arf6 via the recruitment of ACAP2, which inhibits integrin recycling and cell migration. *$P<0.05$, **$P<0.01$.

extensive formation of lammelipodia, indicative of enhanced migration and invasion capabilities (Radisky et al., 2005; Yilmaz and Christofori, 2009). Indeed, we observe that Rab35 knock down also alters cell morphology: cells show a loss of actin stress fibres and have membrane ruffling with formation of multiple actin and β1-integrin-rich lamellipodia-like structures (supplementary material Fig. S4A,B). In addition, enhanced activity of Arf6 is linked to the oncogenic effect of EGF receptor in breast and lung cancers (Sabe et al., 2009; Morishige et al., 2008) and EGF receptor is overexpressed or mutated to become constitutively active in many forms of cancer (CGARN, 2008). Finally, enhanced proliferation and migration, coupled with decreased intercellular adhesion are hallmarks of malignant tumor cells. We thus speculated that Rab35 expression levels would be reduced in tumors. Using qRT-PCR, we find that Rab35 mRNA expression is suppressed in high-grade gliomas, and in breast and squamous cancers (Fig. 5A–C). In contrast, the levels of Arf6 mRNA are not significantly modified (Fig. 5A–C); however, our data on the suppression of Arf6 activity by Rab35 is consistent with the notion that the downregulation of Rab35 levels in tumors directly contributes to the cancer aspects driven by Arf6 hyperactivity.

Discussion

Early/sorting endosomes are highly dynamic compartments that constantly receive material internalized by various endocytic pathways while simultaneously sorting cargo for retention, recycling or degradation. The mechanisms governing cargo selection towards degradation in lysosomes are the best understood of the endosomal sorting decisions, involving a sequential transition from Rab5 to Rab7 on endosomal membranes (Rink et al., 2005; Poteryaev et al., 2010). Lately, such Rab cascades have become an attractive model to explain how trafficking pathways assure linearity of cargo transport (Hutagalung and Novick, 2011). However, a linear Rab cascade cannot insure coordination of trafficking pathways leading to antagonistic functions. Here, we discover that the mutually exclusive trafficking routes mediating recycling and function of

Journal of Cell Science

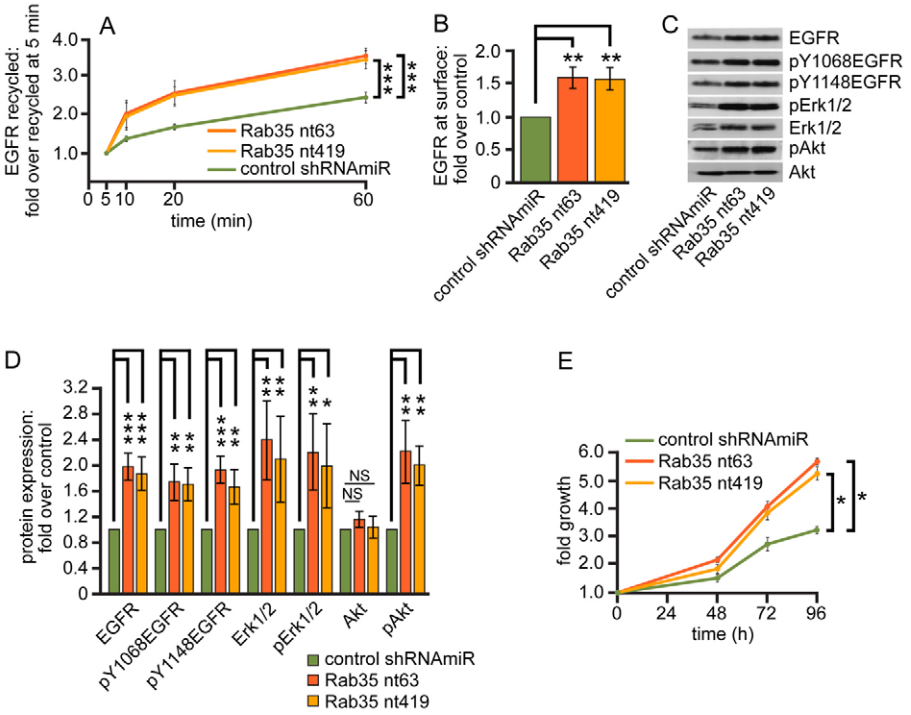

Fig. 4. Rab35 knock down enhances EGF receptor signaling. (**A–F**) For all panels, COS-7 cells were treated with control shRNAmiR or two different shRNAmiRs targeting Rab35 (Rab35 nt63 and Rab35 nt419) as indicated. (A) Quantification of the recycling of EGF receptor measured by FACS. Experiments and quantification were performed as in Fig. 2D. Data represents four duplicate experiments. Error bars are s.e.m. and statistical analysis employed a repeated-measure two-way ANOVA followed by a Bonferroni post-test. (B) Quantification of the surface pool of EGF receptor. Experiments and quantification were performed as in Fig. 2E. Error bars represent s.d. and statistical analysis employed a repeated-measure one-way ANOVA followed by a Dunnett's post-test. (C) Cell lysates were processed for western blot with antibodies recognizing EGF receptor (EGFR), EGF receptor phosphorylated on tyrosine 1068 or 1148, and Erk and Akt or the active, phosphorylated forms of these kinases. (D) Quantification of four experiments performed as in C. The graph shows the average fold change in signal in Rab35 knock down cells relative to control cells. Error bars represent s.d. and statistical analysis employed a repeated-measure one-way ANOVA followed by a Dunnett's post-test. (E) Cells were plated in 96-well plates at 1000 cells per well. Cell growth at indicated time point represents fold change relative to time 0. The graph represents eight repeats from three separate experiments. Error bars represent s.e.m. Statistical analysis employed a repeated-measure two-way ANOVA followed by a Bonferroni post-test. *P<0.05, **P<0.01, ***P<0.001; NS, not significant.

cadherins and integrins are coordinated by a molecular module involving the small GTPases Rab35 and Arf6, which inhibit each other's activities.

In this antagonistic module, active Rab35 promotes cell–cell adhesion by maintaining cadherins at the cell surface, likely by directly guiding their recycling. Knock down of Rab35 leads to cadherin accumulation in endosomes, decreased cadherin surface levels and reduced cell–cell adhesion. Simultaneously, active Rab35 recruits its effector, the Arf6 GAP ACAP2 to inhibit the function of Arf6. Knock down of Rab35 alleviates ACAP2-mediated downregulation of Arf6 activity, leading to enhanced activation of Arf6. This in turn increases Arf6-dependent

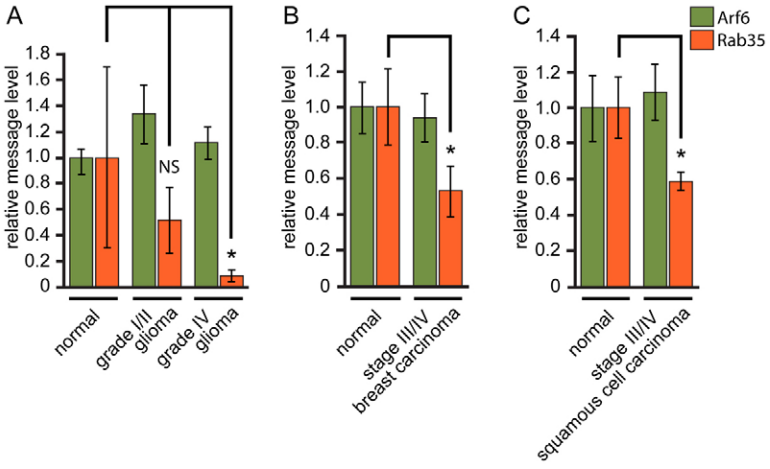

Fig. 5. Rab35 expression is decreased in human tumors. For all panels, the relative mRNA levels for Rab35 and Arf6 were quantified from surgically resected human tumors and normal control tissue from the same patient. (**A**) 19 normal, 13 grade I/II and 24 grade IV gliomas; (**B**) 14 normal and 15 stage III/IV breast carcinoma; and (**C**) 14 normal and 13 stage III/IV squamous cell carcinoma. Error bars represent s.e.m. and statistical analysis employed a repeated-measure one-way ANOVA followed by a Dunnett's post-test. *P<0.05; NS, not significant.

Journal of Cell Science

recycling of β1-integrin, causing increased receptor levels with consequent enhancement of β1-integrin signaling and cell migration. Importantly, depletion of Arf6 expression in Rab35 knock down cells blocks the enhanced cell migration seen with Rab35 knock down alone, demonstrating that Rab35 controls the activity level of Arf6 to indirectly modulate β1-integrin recycling and cell migration. *In vivo*, the Rab35/Arf6 module would provide a mechanism for cells to switch from a motile state to one allowing for cell–cell interaction and differentiation. It is worth noting that in our previous study Rab35 knock down did not influence β1-integrin recycling (Allaire et al., 2010). However, there were several important differences in experimental approach. First, unlike the previous study, here we did not serum-starve the cells prior to labeling surface β1-integrin and thus did not sensitize cells to growth factors from the media that are known to stimulate integrin recycling via Arf6, and which could reduce the inhibitory effect of Rab35 on Arf6 in wild-type cells preventing detection of the influence of Rab35 knock down. Second, in the current study we designed our recycling assay to enhance the sensitivity to resurfacing receptor instead of detecting receptor retained in the cell. In addition, we followed resurfacing receptor over time, which gave a more precise measure of the recycling kinetics, whereas we previously determined the amount of β1-integrin retained at 2 hours only, a point at which the system could have already achieved equilibrium.

Given that active Arf6 binds the Rab35 GAPs TBC1D10A (Hanono et al., 2006), TBC1D10B (Chesneau et al., 2012), and TBC1D24/Skywalker (Uytterhoeven et al., 2011), it seems highly likely that the ability of receptor tyrosine kinases such as EGF, human growth hormone and VEGF receptors to activate Arf6 leading to removal of cell surface cadherins (Palacios et al., 2001; Lu et al., 2003; Morishige et al., 2008; Sabe et al., 2009; Ji et al., 2009; Hashimoto et al., 2011) is mediated through inhibition of Rab35 activity. Moreover, active Arf6 inhibits MHC class I recycling (Caplan et al., 2002; Naslavsky et al., 2004) and we previously demonstrated that knock down of Rab35 inhibits efficient MHC class I recycling (Allaire et al., 2010). Thus, active Arf6 reduces the activity level of Rab35, which interferes with the efficient recycling of various Rab35-dependent receptor cargos. As such, Rab35 and Arf6 form a mutually antagonistic module. Interestingly, the mutual antagonism likely extends beyond the recruitment of respective GAPs. The acidic C-terminal tail of Rab35 directs the GTPase to PtdIns(4,5)P_2-rich membranes such as the plasma membrane and Arf6-positive endosomes (Heo et al., 2006; Kouranti et al., 2006; Chesneau et al., 2012). Arf6 activity catalyzes the production of PtdIns(4,5)P_2 by recruiting the effector PtdIns-kinases PIP5a, b and c (Funakoshi et al., 2011) and this may support co-localization of Rab35 to Arf6 compartments. Intriguingly, Rab35 itself recruits the PtdIns5P phosphatase OCRL (Dambournet et al., 2011) converting PtdIns(4,5)P_2 to PtdIns4P, countering Arf6-mediated PtdIns(4,5)P_2 formation. Thus, lipid-modifying effectors of Rab35 and Arf6 also assure the generation of specific recycling pathways by enhancing the production of either PtdIns4P by Rab35 or PtdIns(4,5)P_2 by Arf6. This would increase the likelihood that only one set of lipid-interacting proteins is recruited in sufficient amounts at any given time. Moreover, the Arf6 effector EPI64 also functions as a GAP for Rab8 and regulates Arf6-dependent membrane trafficking (Hokanson and Bretscher, 2012) indicating that this type of interplay extends to other Arf6/Rab pairs.

Uncontrolled Arf6 activity resulting from overexpression or kinase-activating mutations in EGF receptor drive proliferation and invasion in malignant brain tumors (Li et al., 2006; Li et al., 2009; Hu et al., 2009), squamous cell carcinomas (Menju et al., 2011), and breast cancer (Hashimoto et al., 2006; Morishige et al., 2008). A role for Arf6 in driving tumor formation has also been shown *in vivo* using xenografts in nude mice (Muralidharan-Chari et al., 2009). Here, we demonstrate that release of Rab35/ACAP2-mediated inhibition of Arf6 increases the activity of Arf6 and in turn leads to increased recycling of both β1-integrin and EGF receptor. To our surprise, we also noticed a strong increase in β1-integrin and EGF receptor expression levels, which has not been reported as a consequence of increased Arf6 activity. This is likely because previous studies used expression of mutant forms of Arf6 that disrupt the GTPase cycle, which impedes both endocytosis and recycling by sequestering GEFs, GAPs and effectors. Thus, our results reveal a novel Arf6 function in which activation of endogenous Arf6 increases β1-integrin and EGF receptor expression levels by rerouting them from the degradation pathway to a recycling pathway. This triggers enhanced signaling from Erk1/2, Akt and FAK, core signaling pathways that promote proliferation and accordingly, we observe enhanced proliferation rates, an additional hallmark of cancer. Interestingly, Erk1/2 and FAK also directly disrupt cadherin-based junctions by phosphorylating α-catenin (Ji et al., 2009) and β-catenin (Chen et al., 2012), respectively. These phosphorylation events disrupt interactions of cadherin with cortical actin, which are required for stable cell–cell junctions (reviewed in Stepniak et al., 2009). As a result, Rab35 and Arf6 likely control cell adhesive properties not only via trafficking but also through modulation of signaling kinases.

To further validate the pathophysiological implications of the Rab35/Arf6 module, we determined Rab35 levels in brain, breast and squamous tumors, which are all associated with EGF receptor overexpression and enhanced Arf6 activity. Importantly, we found a strong reduction in Rab35 expression levels in the high-grade tumors. This reduction was most notable in high-grade malignant gliomas, which are highly invasive leading to extremely poor prognosis. As a result, our *in vitro* phenotypes observed upon Rab35 knock down are entirely consistent with the overwhelming bulk of information correlating tumor aggressiveness with EGF receptor expression, kinase signaling, proliferation and invasion, providing a first comprehensive explanation of all phenotypes.

To conclude, our study has determined how two seemingly separate recycling pathways that traffic distinct cargos are coordinated to appropriately regulate antagonistic cell functions. In this scheme, we find that the combination of specific cargo recycling and mutual antagonistic activity between Arf6 and Rab35 allows for control of each other's feed-forward loops to coordinate integrin and cadherin function required for migration and differentiation. Given the importance of Arf6 hyperactivity in tumor invasive properties and the downregulation of Rab35 in tumors, it is likely that manipulation of the Rab35/Arf6 module, for example through upregulation of Rab35 activity, would have efficacy in the treatment of highly aggressive tumors such as gliomas, which currently have an extremely poor prognosis.

Journal of Cell Science

Materials and Methods

Antibodies and fluorophores

Mouse monoclonal antibodies recognizing EGF receptor (SC-120), MHC class I (W6/32) and β1-integrin (TS2/16) were from Santa Cruz Biotechnology Inc. (Santa Cruz, CA), FLAG (M2) was from Sigma (St Louis, MO), Erk1/2 (3A7) and pErk1/2 (E10) from Cell Signaling (Danvers, MA), and FAK from Millipore (Temecula, CA). Rabbit polyclonal antibodies recognizing GFP (A6455) and pY397-FAK (44624G) were from Invitrogen (Carlsbad, CA), c-myc (C-3959) and pan-cadherin (C3678) were from Sigma, Arf6 (Ab77581) and β1-integrin (Ab52971) were from Abcam (Cambridge, MA), EGF receptor (1005) from Santa Cruz, and Akt (9272), pT308-Akt (9275), pY1068-EGF receptor (D7A5), and pY1148-EGF were from Cell Signaling. Polyclonal antibodies against CLCs, connecdenn 1 (3776), and Rab35 have been described previously (Allaire et al., 2006; Poupon et al., 2008; Allaire et al., 2010). Alexa-Fluor-647-EGF and phalloidin-TRITC were from Invitrogen.

Expression constructs

Human ACAP2 (NM_006861) was obtained from Open Biosystems. The coding sequences was amplified by PCR and cloned into pcDNA3-FLAG. Rab35 wild type, S22N and Q67L in pGEX-6P1-GST and Rab35 wild-type in pEGFP-C1 and pcDNA3-FLAG were previously described (Allaire et al., 2010). GST-GGA3 (aa 1–316) was generously provided by J. Bonifacino (NIH). Arf6-HA was generated by L. Santy (Pennsylvania State University) and was obtained from Addgene and non-tagged E-cadherin was provided by D. Colman (Montreal Neurological Institute). All plasmids were verified by sequencing.

Immunofluorescence

COS-7 cells were plated on poly-L-lysine-coated coverslips and transfected 24 hours later using JetPrime (Polyplus Transfection; Illkirch, France) following the manufacturer's recommendations. Following overnight incubation, cells were fixed in 4% PFA and processed for immunofluorescence following standard protocols.

Knock down of Rab35 and Arf6

Knock down of Rab35 was performed as previously described (Allaire et al., 2010). Target sequences for Arf6 were designed using the Block-iT RNAi Designer (Invitrogen) and the human Arf6 mRNA sequence NM_001663.3 (Arf6 nt428, TCAAGTTGTGCGGTCGGTGAT; Arf6 nt693, CGGCAAGACAACAATCCTG-TA) and oligonucleotides were subcloned into pcDNA6.2/GW-EmGFP-miR (Invitrogen) to yield shRNAmiR knock down constructs. Viral particles were prepared in HEK-293T cells, concentrated by centrifugation and titered using HEK-293T cells as previously described (Thomas et al., 2009; Allaire et al., 2010). The control shRNAmiR virus was described previously (Thomas et al., 2009). For knock down studies in COS-7 cells, cells were plated on the day of transduction and viruses were added at a multiplicity of infection (MOI) of 7.5. The next day media was replaced with fresh culture medium. For subsequent Arf6 knock down, Rab35 knock down cells were plated on the day of transduction (1 week after transduction by Rab35 viruses or control viruses) and viruses targeting Arf6 were added at a MOI of 7.5. The next day, media was replaced with fresh culture media. In all experiments, data was obtained from at least two different viral preparations and three transductions. All experiments were performed 7–21 days post transduction.

Rescue experiments

For the rescue of Rab35 expression, mouse Rab35 was cloned in frame in a pRRLsinPPT plasmid in which the sequence that is used to accept the microRNA sequence downstream of the emGFP expression cassette was replaced with a polylinker. This construct was then used to transduce (MOI of 4) Rab35 knock down cells (human Rab35 targeting sequence) generating emGFP-Rab35 expressing cells.

GST-Rab35 affinity-selection assays

FLAG-tagged ACAP2 was expressed in HEK-293T cells that were lysed in 10 mM HEPES pH 7.4, 100 mM NaCl supplemented with protease inhibitors (0.83 mM benzamidine, 0.23 mM phenylmethylsulphonyl fluoride, 0.5 μg/ml aprotinin and 0.5 μg/ml leupeptin). Triton X-100 was added to a final concentration of 1% and lysates were rocked for 5 minutes at 4℃ before centrifugation at 205,000 ***g*** to remove insoluble material. Aliquots of the supernatant were incubated for 1 hour at 4℃ with 10 μg of GST-Rab35 (wild type, Q67L or S22N) fusion proteins and then washed with lysis buffer containing 1% Triton X-100. Proteins specifically bound to the beads were analyzed by SDS-PAGE and western blot.

Quantification of Arf6-GTP in cells

Transduced COS-7 cells were grown to 70% confluency in 15 cm dishes and lysed in 50 mM Tris pH 7.4, 200 mM NaCl, 10 mM $MgCl_2$, 1% Triton, 0.5% deoxycholate, 0.1% SDS, and 5% glycerol supplemented with protease inhibitors. Lysates were centrifuged for 5 minutes at 4℃ at 205,000 ***g***. A 4 mg aliquot of the supernatant was incubated with 40 μg of GST-GGA3 (aa 1–316) for 1 hour and washed three times with lysis buffer. Proteins specifically bound to the beads were analyzed by SDS-PAGE and western blot.

Surface biotinylation assays

Cells at 100% confluency in 6 well dishes were washed three times with ice cold PBS containing 1 mM $MgCl_2$ and 0.1 mM $CaCl_2$. Cells were then incubated for 30 minutes on ice with 0.5 mg/ml EZ-link sulfo-NHS-LC-biotin (Pierce, Thermo Scientific). Cells were subsequently washed 2 times in PBS containing 1 mM $MgCl_2$, 0.1 mM $CaCl_2$ and were then incubated in PBS containing 1 mM $MgCl_2$, 0.1 mM $CaCl_2$ and 10 mM glycine. Cells were lysed on ice with 1.5 ml of lysis buffer (50 mM Tris pH 7.4, 200 mM NaCl, 1% Triton, 0.5% deoxycholate, 0.1% SDS, 5% glycerol, supplemented with protease inhibitors). Cell lysates were harvested with a rubber policeman, passed through a 26 gauge needle three times and centrifuged at 205,000 ***g*** at 4℃ for 5 minutes to remove insoluble material. Aliquots of protein lysates (200 μg) were incubated with streptavidin-coupled agarose beads (Pierce, Thermo Scientific) for 1 hour and washed four times with lysis buffer. Samples were separated by SDS-PAGE and levels of cadherin were detected by western blot.

β1-integrin and EGF receptor surface expression analysis

Transduced cells were incubated with 1 μg of anti-β1-integrin or anti-EGF receptor antibodies per 10^6 cells for 1 hour at 4℃ in DMEM, washed three times with ice cold PBS, and were then incubated with Alexa-Fluor-647-conjugated secondary antibody (1:500) in PBS at 4℃ for 30 minutes. The cells were washed with PBS, removed from the plate in 1 ml of PBS using a rubber policeman, filtered through a cell strainer, and analyzed immediately by flow cytometry on a FACSCalibur (Becton Dickinson). In each assay, 10,000 cells were analyzed for each time point (in duplicate).

β1-integrin and EGFR recycling assays

Transduced cells were incubated with 1 μg of anti-β1-integrin or anti-EGF receptor antibodies per 10^6 cells for 2 hours at 37℃ in DMEM. Cells were then chilled on ice and surface-bound antibody was removed by acid wash (0.5 M NaCl, 0.2 M acetic acid, pH 2.5) followed by a PBS wash. Cells were then incubated in pre-warmed DMEM plus 10% serum containing Alexa-Fluor-647-conjugated secondary antibody (1:500) at 37℃. At the indicated time points, cells were chilled to 4℃, washed with PBS, scraped off the plates, and processed by flow cytometry. In each assay, 10,000 cells were analyzed for each time point (in duplicate). Each time point represents the fold recycling over the 5-minute time point.

Cell proliferation assays

Cell proliferation assays (MTT assays) were performed as described (Maret et al., 2010). Briefly, cells were seeded in 96-well plates at 1000 cells/well and MTT (Sigma-Aldrich) was added at a final concentration of 0.5 mg/ml at different time points. The plates were incubated at 37℃ for 4 hours, the medium was then removed, 100 μl of DMSO was added per well, plates were incubated at 37℃ for 1 hour, and the absorption was measured at 595 nm using a spectrophotometer. The optical density of the sample was subtracted from that of the blank. An exponential growth trend line was applied to the data points yielding the following equation: $Y(t)=Y_0e^{kt}$ where $Y(t)$ is the optical density at 595 nm at time point t, Y_0 is the optical density at $t=0$, k is the growth constant, and t is time. The doubling time (t_d) was calculated using the equation $t_d=\ln 2/k$.

Cell aggregation assay

Aggregation assays were performed as described (Maret et al., 2010). Briefly, monolayer cultures were treated with 2 mM EDTA in PBS for 5 minutes at 37℃ to invoke cadherin internalization and cell dissociation. Cells were then pelleted to removed EDTA and resuspended in DMEM with 10% bovine calf serum until cells were visibly completely dissociated and 5×10^5 cells were seeded at a final volume of 0.5 ml per well, and transferred onto 24-well low-adherent plates (VWR, Mississauga, Ontario, Canada). The plates were set on an orbital shaker at 80 rpm at 37℃ to allow aggregation. Samples were taken from individual wells at different time points and immediately examined by light microscopy. The assay was quantified as follows: The number of single cells was measured at different time points and the rate of aggregation at time t was calculated as the ratio of single cells/total cells.

Wound healing migration assays

The two-dimensional migration of cell lines was assayed by wound healing migration as previously described (Maret et al., 2010). Briefly 2.2×10^5 cells were seeded in 12-well cell culture plates and grown to confluency. The wells were marked on the underside (serving as fiducial marks for analysis of wound areas). The culture media was removed and replaced by PBS and monolayers were disrupted with a parallel scratch wound made with a fine pipette tip. Migration into the wound was observed using phase-contrast microscopy on an inverted microscope with the 5× objective. Images of the wound were taken at regular

time intervals. The number of cells that migrated into the wound was counted using Northern Eclipse software 6.0 (EMPIX Imaging, Inc., Mississauga, Ontario, Canada).

Human tissues

Human brain tumor samples were obtained from the Montreal Neurological Institute Brain Tumor Tissue Bank. The experimental procedures were approved by the ethics committee of the Montreal Neurological Institute. The breast and squamous cell carcinomas and normal tissues were obtained from FolioBio (Columbus, OH).

RNA extraction, cDNA synthesis and real-time quantitative PCR

RNA was extracted from frozen human tissue using the RNeasy kit (Qiagen, Missisauga, Ontario, Canada) following manufacturer's recommendations. The RNeasy FFPE kit was used for the RNA extraction of paraffin-embedded tissue samples (Qiagen, Mississauga, Ontario, Canada) following the manufacturer's recommendations. Typically, 0.5–1 μg of total RNA was used for the first-strand cDNA synthesis using the Superscript cDNA kit (Life Technologies) following the manufacturer's recommendations. qRT-PCR was performed using a Light Cycler (Roche). Reactions (20 μl) contained 2 μl of FastStart DNA Master Mix SYBR Green I, 0.5 μM of the primers and 1 μl of first-strand synthesized template DNA. Primer sequences used in this study are as follows: Rab35, Fw 5′-TCAAGCT-GCTCATCATCGGCGA-3′, Re 5′-CCCCGTTGATCTCCACGGTCC-3′; Arf6, Fw 5′-ATGGGGAAGGTGCTATCCAAAATC-3′, Re 5′-GCAGTCCACTACG-AAGATGAGACC-3′; hs14 control; Fw 5′-CAGGTCCAGGGGTCTTGGTCC-3′, Re 5′-GGCAGACCGAGATGAATCCTCA-3′.

Statistical analysis

Descriptive statistics were analyzed using GraphPad Prism 4. Mean, s.e.m. and Student's *t*-test were used to determine significant differences between pairs. Comparisons of three or more groups were performed using a parametric analysis of variance (ANOVA) and Bonferroni or Dunnett multiple comparison tests. $P<0.05$ was considered significant.

Acknowledgements

We thank R. Biervig (University of Bergen, Norway) for providing the U251 malignant glioma cell line, J. Bonifacino (NIH, USA) for the GST-GGA3 construct, and D. Colman (Montreal Neurological Institute, Canada) for the E-cadherin construct. We also thank the Franco Di Giovanni and Tony Colannino Foundations for support.

Author contributions

P.D.A. helped conceive the study, designed, conducted and interpreted experiments, and helped write the manuscript. M.S.S. helped conceive the study, designed, conducted and interpreted experiments, and helped write the manuscript. M.C. conceived, designed, conducted and interpreted experiments, and helped write the manuscript. E.S.S. conducted and interpreted experiments. S.K. conducted and interpreted experiments. M.F. conducted experiments. D.M. supplied and validated important samples. B.R. helped conceive the study and write the manuscript. R.F.D.M. helped conceive the study and provided and validated important samples. P.S.M. helped conceive the study, conceived, designed and interpreted experiments, and helped write the manuscript.

Funding

This work was supported by the Canadian Institutes of Health Research [grant number MOP15396 to P.S.M.]. M.S.S. holds a C. Geada Brain Tumor Research Fellowship. R.F.D.M. is the W. Feindel Chair in Neuro-Oncology and P.S.M. is a James McGill Professor.

Supplementary material available online at
http://jcs.biologists.org/lookup/suppl/doi:10.1242/jcs.112375/-/DC1

References

Allaire, P. D., Ritter, B., Thomas, S., Burman, J. L., Denisov, A. Y., Legendre-Guillemin, V., Harper, S. Q., Davidson, B. L., Gehring, K. and McPherson, P. S. (2006). Connecdenn, a novel DENN domain-containing protein of neuronal clathrin-coated vesicles functioning in synaptic vesicle endocytosis. *J. Neurosci.* **26**, 13202-13212.

Allaire, P. D., Marat, A. L., Dall'Armi, C., Di Paolo, G., McPherson, P. S. and Ritter, B. (2010). The Connecdenn DENN domain: a GEF for Rab35 mediating cargo-specific exit from early endosomes. *Mol. Cell* **37**, 370-382.

Arjonen, A., Alanko, J., Veltel, S. and Ivaska, J. (2012). Distinct recycling of active and inactive β1 integrins. *Traffic* [Epub ahead of print] doi: 10.1111/j.1600-0854.2012.01327.

Blindt, R., Bosserhoff, A. K., Dammers, J., Krott, N., Demircan, L., Hoffmann, R., Hanrath, P., Weber, C. and Vogt, F. (2004). Downregulation of N-cadherin in the neointima stimulates migration of smooth muscle cells by RhoA deactivation. *Cardiovasc. Res.* **62**, 212-222.

Cancer Genome Atlas Research Network (2008). Comprehensive genomic characterization defines human glioblastoma genes and core pathways. *Nature* **455**, 1061-1068.

Caplan, S., Naslavsky, N., Hartnell, L. M., Lodge, R., Polishchuk, R. S., Donaldson, J. G. and Bonifacino, J. S. (2002). A tubular EHD1-containing compartment involved in the recycling of major histocompatibility complex class I molecules to the plasma membrane. *EMBO J.* **21**, 2557-2567.

Caswell, P. T., Chan, M., Lindsay, A. J., McCaffrey, M. W., Boettiger, D. and Norman, J. C. (2008). Rab-coupling protein coordinates recycling of α5β1 integrin and EGFR1 to promote cell migration in 3D microenvironments. *J. Cell Biol.* **183**, 143-155.

Chen, X. L., Nam, J. O., Jean, C., Lawson, C., Walsh, C. T., Goka, E., Lim, S. T., Tomar, A., Tancioni, I., Uryu, S. et al. (2012). VEGF-induced vascular permeability is mediated by FAK. *Dev. Cell* **22**, 146-157.

Chesneau, L., Dambournet, D., Machicoane, M., Kouranti, I., Fukuda, M., Goud, B. and Echard, A. (2012). An ARF6/Rab35 GTPase cascade for endocytic recycling and successful cytokinesis. *Curr. Biol.* **22**, 147-153.

Dambournet, D., Machicoane, M., Chesneau, L., Sachse, M., Rocancourt, M., El Marjou, A., Formstecher, E., Salomon, R., Goud, B. and Echard, A. (2011). Rab35 GTPase and OCRL phosphatase remodel lipids and F-actin for successful cytokinesis. *Nat. Cell Biol.* **13**, 981-988.

Delva, E. and Kowalczyk, A. P. (2009). Regulation of cadherin trafficking. *Traffic* **10**, 259-267.

Frasa, M. A., Maximiano, F. C., Smolarczyk, K., Francis, R. E., Betson, M. E., Lozano, E., Goldenring, J., Seabra, M. C., Rak, A., Ahmadian, M. R. et al. (2010). Armus is a Rac1 effector that inactivates Rab7 and regulates E-cadherin degradation. *Curr. Biol.* **20**, 198-208.

Funakoshi, Y., Hasegawa, H. and Kanaho, Y. J. (2011). Regulation of PIP5K activity by Arf6 and its physiological significance. *J. Cell Physiol.* **226**, 888-895.

Gao, Y., Balut, C. M., Bailey, M. A., Patino-Lopez, G., Shaw, S. and Devor, D. C. (2010). Recycling of the Ca2+-activated K+ channel, KCa2.3, is dependent upon RME-1, Rab35/EPI64C, and an N-terminal domain. *J. Biol. Chem.* **285**, 17938-17953.

Gu, Z., Noss, E. H., Hsu, V. W. and Brenner, M. B. (2011). Integrins traffic rapidly via circular dorsal ruffles and macropinocytosis during stimulated cell migration. *J. Cell Biol.* **193**, 61-70.

Hanono, A., Garbett, D., Reczek, D., Chambers, D. N. and Bretscher, A. (2006). EPI64 regulates microvillar subdomains and structure. *J. Cell Biol.* **175**, 803-813.

Hashimoto, S., Onodera, Y., Hashimoto, A., Tanaka, M., Hamaguchi, M., Yamada, A. and Sabe, H. (2004). Requirement for Arf6 in breast cancer invasive activities. *Proc. Natl. Acad. Sci. USA* **101**, 6647-6652.

Hashimoto, S., Hirose, M., Hashimoto, A., Morishige, M., Yamada, A., Hosaka, H., Akagi, K., Ogawa, E., Oneyama, C., Agatsuma, T. et al. (2006). Targeting AMAP1 and cortactin binding bearing an atypical src homology 3/proline interface for prevention of breast cancer invasion and metastasis. *Proc. Natl. Acad. Sci. USA* **103**, 7036-7041.

Hashimoto, A., Hashimoto, S., Ando, R., Noda, K., Ogawa, E., Kotani, H., Hirose, M., Menju, T., Morishige, M., Manabe, T. et al. (2011). GEP100-Arf6-AMAP1-cortactin pathway frequently used in cancer invasion is activated by VEGFR2 to promote angiogenesis. *PLoS ONE* **6**, e23359.

Heo, W. D., Inoue, T., Park, W. S., Kim, M. L., Park, B. O., Wandless, T. J. and Meyer, T. (2006). PI(3,4,5)P3 and PI(4,5)P2 lipids target proteins with polybasic clusters to the plasma membrane. *Science* **314**, 1458-1461.

Hokanson, D. E. and Bretscher, A. P. (2012). EPI64 interacts with Slp1/JFC1 to coordinate Rab8a and Arf6 membrane trafficking. *Mol. Biol. Cell* **23**, 701-715.

Hsu, V. W. and Prekeris, R. (2010). Transport at the recycling endosome. *Curr. Opin. Cell Biol.* **22**, 528-534.

Hsu, C., Morohashi, Y., Yoshimura, S., Manrique-Hoyos, N., Jung, S., Lauterbach, M. A., Bakhti, M., Grønborg, M., Möbius, W., Rhee, J. et al. (2010). Regulation of exosome secretion by Rab35 and its GTPase-activating proteins TBC1D10A-C. *J. Cell Biol.* **189**, 223-232.

Hu, B., Shi, B., Jarzynka, M. J., Yiin, J. J., D'Souza-Schorey, C. and Cheng, S. Y. (2009). ADP-ribosylation factor 6 regulates glioma cell invasion through the IQ-domain GTPase-activating protein 1-Rac1-mediated pathway. *Cancer Res.* **69**, 794-801.

Hutagalung, A. H. and Novick, P. J. (2011). Role of Rab GTPases in membrane traffic and cell physiology. *Physiol. Rev.* **91**, 119-149.

Huttenlocher, A., Lakonishok, M., Kinder, M., Wu, S., Truong, T., Knudsen, K. A. and Horwitz, A. F. (1998). Integrin and cadherin synergy regulates contact inhibition of migration and motile activity. *J. Cell Biol.* **141**, 515-526.

Jakob, T. and Udey, M. C. (1998). Regulation of E-cadherin-mediated adhesion in Langerhans cell-like dendritic cells by inflammatory mediators that mobilize Langerhans cells in vivo. *J. Immunol.* **160**, 4067-4073.

Ji, H., Wang, J., Nika, H., Hawke, D., Keezer, S., Ge, Q., Fang, B., Fang, X., Fang, D., Litchfield, D. W. et al. (2009). EGF-induced ERK activation promotes CK2-

Journal of Cell Science

mediated disassociation of alpha-Catenin from beta-Catenin and transactivation of beta-Catenin. *Mol. Cell* **36**, 547-559.

Jones, C. A., Nishiya, N., London, N. R., Zhu, W., Sorensen, L. K., Chan, A. C., Lim, C. J., Chen, H., Zhang, Q., Schultz, P. G. et al. (2009). Slit2-Robo4 signalling promotes vascular stability by blocking Arf6 activity. *Nat. Cell Biol.* **11**, 1325-1331.

Kanno, E., Ishibashi, K., Kobayashi, H., Matsui, T., Ohbayashi, N. and Fukuda, M. (2010). Comprehensive screening for novel rab-binding proteins by GST pull-down assay using 60 different mammalian Rabs. *Traffic* **11**, 491-507.

Kawasaki, M., Nakayama, K. and Wakatsuki, S. (2005). Membrane recruitment of effector proteins by Arf and Rab GTPases. *Curr. Opin. Struct. Biol.* **15**, 681-689.

Kobayashi, H. and Fukuda, M. (2012). Rab35 regulates Arf6 activity through centaurin β2/ACAP2 during neurite outgrowth. *J. Cell Sci.* **125**, 2235-2243.

Kong, D., Banerjee, S., Ahmad, A., Li, Y., Wang, Z., Sethi, S. and Sarkar, F. H. (2010). Epithelial to mesenchymal transition is mechanistically linked with stem cell signatures in prostate cancer cells. *PLoS ONE* **5**, e12445.

Kouranti, I., Sachse, M., Arouche, N., Goud, B. and Echard, A. (2006). Rab35 regulates an endocytic recycling pathway essential for the terminal steps of cytokinesis. *Curr. Biol.* **16**, 1719-1725.

Lenferink, A. E. G., Pinkas-Kramarski, R., van de Poll, M. L., van Vugt, M. J., Klapper, L. N., Tzahar, E., Waterman, H., Sela, M., van Zoelen, E. J. and Yarden, Y. (1998). Differential endocytic routing of homo- and hetero-dimeric ErbB tyrosine kinases confers signaling superiority to receptor heterodimers. *EMBO J.* **17**, 3385-3397.

Li, M., Ng, S. S., Wang, J., Lai, L., Leung, S. Y., Franco, M., Peng, Y., He, M. L., Kung, H. F. and Lin, M. C. (2006). EFA6A enhances glioma cell invasion through ADP ribosylation factor 6/extracellular signal-regulated kinase signaling. *Cancer Res.* **66**, 1583-1590.

Li, M., Wang, J., Ng, S. S., Chan, C. Y., He, M. L., Yu, F., Lai, L., Shi, C., Chen, Y., Yew, D. T. et al. (2009). Adenosine diphosphate-ribosylation factor 6 is required for epidermal growth factor-induced glioblastoma cell proliferation. *Cancer* **115**, 4959-4972.

Lipfert, L., Haimovich, B., Schaller, M. D., Cobb, B. S., Parsons, J. T. and Brugge, J. S. (1992). Integrin-dependent phosphorylation and activation of the protein tyrosine kinase pp125FAK in platelets. *J. Cell Biol.* **119**, 905-912.

Lu, Z., Ghosh, S., Wang, Z. and Hunter, T. (2003). Downregulation of caveolin-1 function by EGF leads to the loss of E-cadherin, increased transcriptional activity of beta-catenin, and enhanced tumor cell invasion. *Cancer Cell* **4**, 499-515.

Marat, A. L. and McPherson, P. S. (2010). The connecdenn family, Rab35 guanine nucleotide exchange factors interfacing with the clathrin machinery. *J. Biol. Chem.* **285**, 10627-10637.

Maret, D., Gruzglin, E., Sadr, M. S., Siu, V., Shan, W., Koch, A. W., Seidah, N. G., Del Maestro, R. F. and Colman, D. R. (2010). Surface expression of precursor N-cadherin promotes tumor cell invasion. *Neoplasia* **12**, 1066-1080.

Margadant, C., Monsuur, H. N., Norman, J. C. and Sonnenberg, A. (2011). Mechanisms of integrin activation and trafficking. *Curr. Opin. Cell Biol.* **23**, 607-614.

Mattoon, D. R., Lamothe, B., Lax, I. and Schlessinger, J. (2004). The docking protein Gab1 is the primary mediator of EGF-stimulated activation of the PI-3K/Akt cell survival pathway. *BMC Biol.* **2**, 24.

Maxfield, F. R. and McGraw, T. E. (2004). Endocytic recycling. *Nat. Rev. Mol. Cell Biol.* **5**, 121-132.

Menju, T., Hashimoto, S., Hashimoto, A., Otsuka, Y., Handa, H., Ogawa, E., Toda, Y., Wada, H., Date, H. and Sabe, H. (2011). Engagement of overexpressed Her2 with GEP100 induces autonomous invasive activities and provides a biomarker for metastases of lung adenocarcinoma. *PLoS ONE* **6**, e25301.

Micalizzi, D. S., Farabaugh, S. M. and Ford, H. L. (2010). Epithelial-mesenchymal transition in cancer: parallels between normal development and tumor progression. *J. Mammary Gland Biol. Neoplasia* **15**, 117-134.

Miura, K., Nam, J. M., Kojima, C., Mochizuki, N. and Sabe, H. (2009). EphA2 engages Git1 to suppress Arf6 activity modulating epithelial cell-cell contacts. *Mol. Biol. Cell* **20**, 1949-1959.

Morishige, M., Hashimoto, S., Ogawa, E., Toda, Y., Kotani, H., Hirose, M., Wei, S., Hashimoto, A., Yamada, A., Yano, H. et al. (2008). GEP100 links epidermal growth factor receptor signalling to Arf6 activation to induce breast cancer invasion. *Nat. Cell Biol.* **10**, 85-92.

Muller, P. A., Caswell, P. T., Doyle, B., Iwanicki, M. P., Tan, E. H., Karim, S., Lukashchuk, N., Gillespie, D. A., Ludwig, R. L., Gosselin, P. et al. (2009). Mutant p53 drives invasion by promoting integrin recycling. *Cell* **139**, 1327-1341.

Muralidharan-Chari, V., Hoover, H., Clancy, J., Schweitzer, J., Suckow, M. A., Schroeder, V., Castellino, F. J., Schorey, J. S. and D'Souza-Schorey, C. (2009). ADP-ribosylation factor 6 regulates tumorigenic and invasive properties in vivo. *Cancer Res.* **69**, 2201-2209.

Naslavsky, N., Boehm, M., Backlund, P. S., Jr and Caplan, S. (2004). Rabenosyn-5 and EHD1 interact and sequentially regulate protein recycling to the plasma membrane. *Mol. Biol. Cell* **15**, 2410-2422.

Palacios, F., Price, L., Schweitzer, J., Collard, J. G. and D'Souza-Schorey, C. (2001). An essential role for ARF6-regulated membrane traffic in adherens junction turnover and epithelial cell migration. *EMBO J.* **20**, 4973-4986.

Palacios, F., Schweitzer, J. K., Boshans, R. L. and D'Souza-Schorey, C. (2002). ARF6-GTP recruits Nm23-H1 to facilitate dynamin-mediated endocytosis during adherens junctions disassembly. *Nat. Cell Biol.* **4**, 929-936.

Patino-Lopez, G., Dong, X., Ben-Aissa, K., Bernot, K. M., Itoh, T., Fukuda, M., Kruhlak, M. J., Samelson, L. E. and Shaw, S. (2008). Rab35 and its GAP EPI64C in T cells regulate receptor recycling and immunological synapse formation. *J. Biol. Chem.* **283**, 18323-18330.

Polyak, K. and Weinberg, R. A. (2009). Transitions between epithelial and mesenchymal states: acquisition of malignant and stem cell traits. *Nat. Rev. Cancer* **9**, 265-273.

Poteryaev, D., Datta, S., Ackema, K., Zerial, M. and Spang, A. (2010). Identification of the switch in early-to-late endosome transition. *Cell* **141**, 497-508.

Poupon, V., Girard, M., Legendre-Guillemin, V., Thomas, S., Bourbonniere, L., Philie, J., Bright, N. A. and McPherson, P. S. (2008). Clathrin light chains function in mannose phosphate receptor trafficking via regulation of actin assembly. *Proc. Natl. Acad. Sci. USA* **105**, 168-173.

Radhakrishna, H., Al-Awar, O., Khachikian, Z. and Donaldson, J. G. (1999). ARF6 requirement for Rac ruffling suggests a role for membrane trafficking in cortical actin rearrangements. *J. Cell Sci.* **112**, 855-866.

Radisky, D. C., Levy, D. D., Littlepage, L. E., Liu, H., Nelson, C. M., Fata, J. E., Leake, D., Godden, E. L., Albertson, D. G., Nieto, M. A. et al. (2005). Rac1b and reactive oxygen species mediate MMP-3-induced EMT and genomic instability. *Nature* **436**, 123-127.

Rahajeng, J., Giridharan, S. S., Cai, B., Naslavsky, N. and Caplan, S. (2012). MICAL-L1 is a tubular endosomal membrane hub that connects Rab35 and Arf6 with Rab8a. *Traffic* **13**, 82-93.

Rink, J., Ghigo, E., Kalaidzidis, Y. and Zerial, M. (2005). Rab conversion as a mechanism of progression from early to late endosomes. *Cell* **122**, 735-749.

Rodrigues, G. A., Falasca, M., Zhang, Z., Ong, S. H. and Schlessinger, J. (2000). A novel positive feedback loop mediated by the docking protein Gab1 and phosphatidylinositol 3-kinase in epidermal growth factor receptor signaling. *Mol. Cell. Biol.* **20**, 1448-1459.

Rojas, M., Yao, S. and Lin, Y. Z. (1996). Controlling epidermal growth factor (EGF)-stimulated Ras activation in intact cells by a cell-permeable peptide mimicking phosphorylated EGF receptor. *J. Biol. Chem.* **271**, 27456-27461.

Sabe, H., Hashimoto, S., Morishige, M., Ogawa, E., Hashimoto, A., Nam, J. M., Miura, K., Yano, H. and Onodera, Y. (2009). The EGFR-GEP100-Arf6-AMAP1 signaling pathway specific to breast cancer invasion and metastasis. *Traffic* **10**, 982-993.

Santy, L. C. and Casanova, J. E. (2001). Activation of ARF6 by ARNO stimulates epithelial cell migration through downstream activation of both Rac1 and phospholipase D. *J. Cell Biol.* **154**, 599-610.

Schweitzer, J. K., Sedgwick, A. E. and D'Souza-Schorey, C. (2011). ARF6-mediated endocytic recycling impacts cell movement, cell division and lipid homeostasis. *Semin. Cell Dev. Biol.* **22**, 39-47.

Shoval, I., Ludwig, A. and Kalcheim, C. (2007). Antagonistic roles of full-length N-cadherin and its soluble BMP cleavage product in neural crest delamination. *Development* **134**, 491-501.

Stepniak, E., Radice, G. L. and Vasioukhin, V. (2009). Adhesive and signaling functions of cadherins and catenins in vertebrate development. *Cold Spring Harb. Perspect. Biol.* **1**, a002949.

Svensson, H. G., West, M. A., Mollahan, P., Prescott, A. R., Zaru, R. and Watts, C. (2008). A role for ARF6 in dendritic cell podosome formation and migration. *Eur. J. Immunol.* **38**, 818-828.

Tague, S. E., Muralidharan, V. and D'Souza-Schorey, C. (2004). ADP-ribosylation factor 6 regulates tumor cell invasion through the activation of the MEK/ERK signaling pathway. *Proc. Natl. Acad. Sci. USA* **101**, 9671-9676.

Thiery, J. P. (2003). Epithelial-mesenchymal transitions in development and pathologies. *Curr. Opin. Cell Biol.* **15**, 740-746.

Thomas, S., Ritter, B., Verbich, D., Sanson, C., Bourbonnière, L., McKinney, R. A. and McPherson, P. S. (2009). Intersectin regulates dendritic spine development and somatodendritic endocytosis but not synaptic vesicle recycling in hippocampal neurons. *J. Biol. Chem.* **284**, 12410-12419.

Uytterhoeven, V., Kuenen, S., Kasprowicz, J., Miskiewicz, K. and Verstreken, P. (2011). Loss of skywalker reveals synaptic endosomes as sorting stations for synaptic vesicle proteins. *Cell* **145**, 117-132.

Walseng, E., Bakke, O. and Roche, P. A. (2008). Major histocompatibility complex class II-peptide complexes internalize using a clathrin- and dynamin-independent endocytosis pathway. *J. Biol. Chem.* **283**, 14717-14727.

Worthylake, R., Opresko, L. K. and Wiley, H. S. (1999). ErbB-2 amplification inhibits down-regulation and induces constitutive activation of both ErbB-2 and epidermal growth factor receptors. *J. Biol. Chem.* **274**, 8865-8874.

Yilmaz, M. and Christofori, G. (2009). EMT, the cytoskeleton, and cancer cell invasion. *Cancer Metastasis Rev.* **28**, 15-33.

Zhang, Q., Calafat, J., Janssen, H. and Greenberg, S. (1999). ARF6 is required for growth factor- and rac-mediated membrane ruffling in macrophages at a stage distal to rac membrane targeting. *Mol. Cell. Biol.* **19**, 8158-8168.

Zwick, E., Hackel, P. O., Prenzel, N. and Ullrich, A. (1999). The EGF receptor as central transducer of heterologous signalling systems. *Trends Pharmacol. Sci.* **20**, 408-412.

Journal of Cell Science

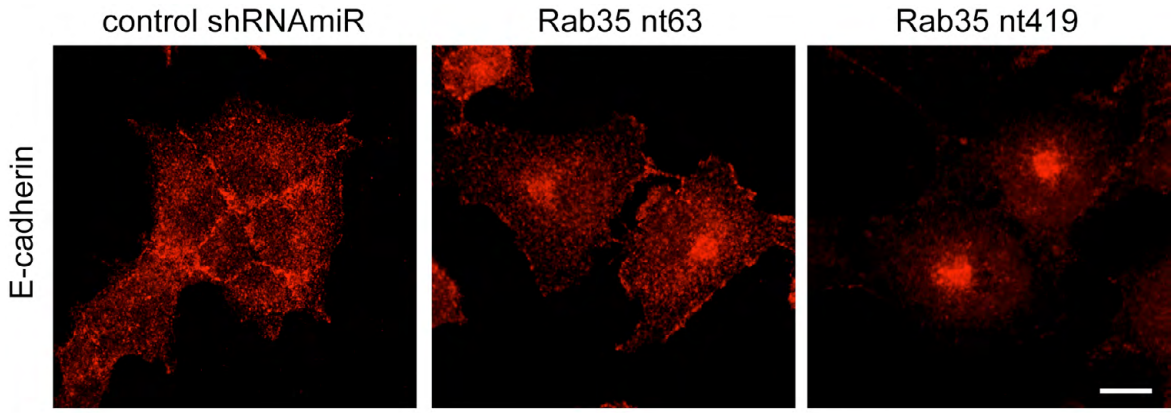

Fig. S1. Rab35 knock down inhibits recycling of E-cadherin. COS-7 cells were treated with control shRNAmiR or two different shRNAmiRs targeting Rab35 (Rab35 nt63 and Rab35 nt419) as indicated. Cells were transfected with Flag-tagged E-cadherin and then stained with an anti-Flag antibody. Scale bar = 10 μm.

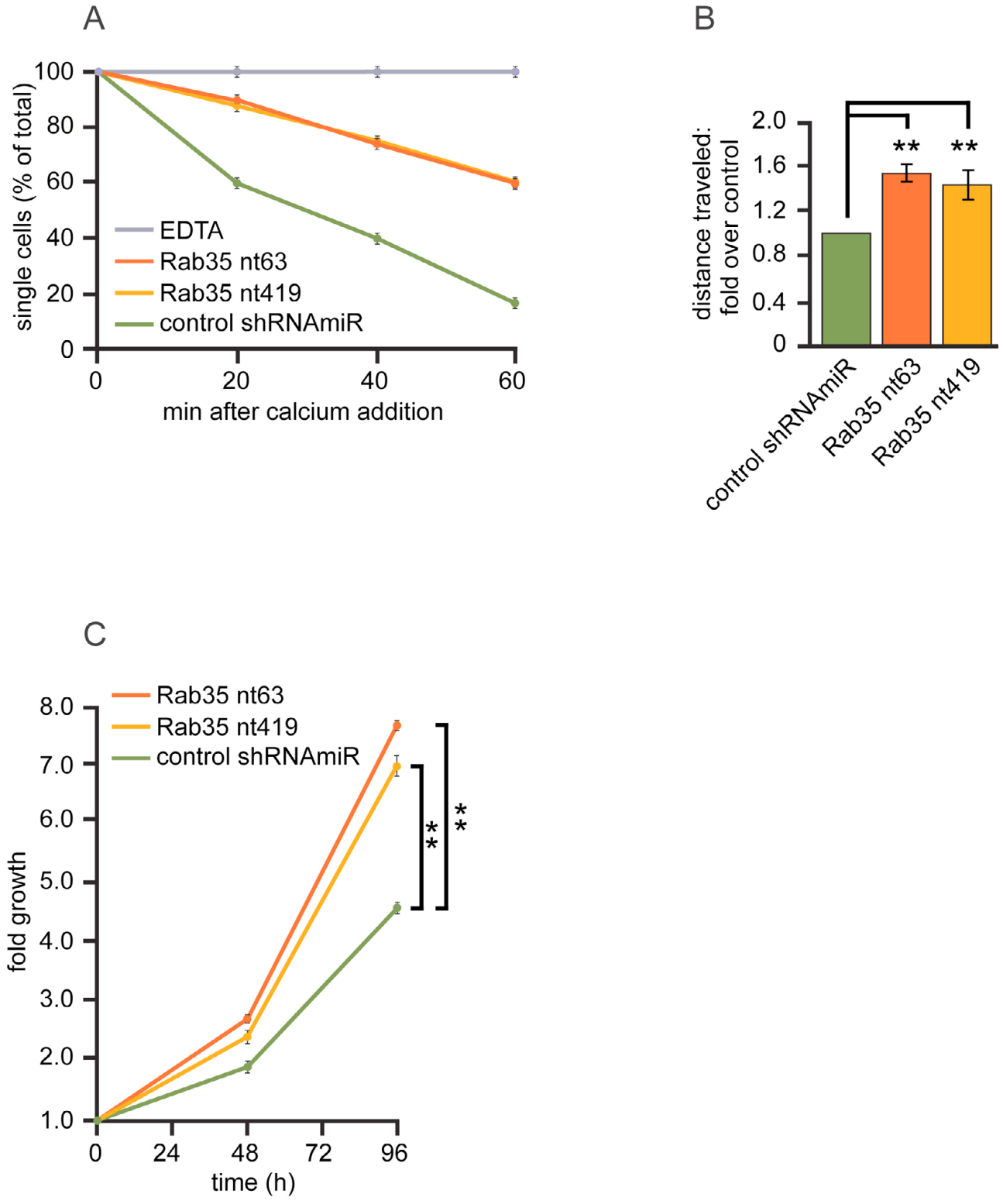

Fig. S2. Adhesion, migration and proliferation of glioblastoma derived U251 cells. (**A-C**) For all panels, U251 glioblastoma-derived cells were treated with control shRNAmiR or two different shRNAmiRs targeting Rab35 (Rab35 nt63 and Rab35 nt419) as indicated. **(A)** Cells were treated with 2 mM EDTA to dissociate monolayers into single cells. The cells were then pelleted, washed and resuspended in Ca^{2+}-containing culture media. Cells were agitated gently and 50 µl aliquots of cell suspension were analyzed at 20 min intervals. Four fields of approximately 200 cells were analyzed per time point from 3 duplicate aggregation assays. Statistical analysis employed a repeated-measure two-way ANOVA followed by a Bonferroni post-test. (**B**) A scratch was made in a confluent monolayer of cells and images were obtained immediately after the scratch and after 16 h. Cell migration into the scratch was determined from 3 duplicate experiments. Error bars represent standard error of the means and statistical analysis employed a repeated-measure one-way ANOVA followed by a Dunnet's post-test (**p<0.01). **(C)** Cells were plated in 96-well plates at 1000 cells per well. Cell growth at indicated time point represents fold change relative to time 0. The graph represents 8 repeats from 3 separate experiments. Error bars represent standard error of the means. Statistical analysis employed a repeated-measure two-way ANOVA followed by a Bonferroni post-test (*p<0.05).

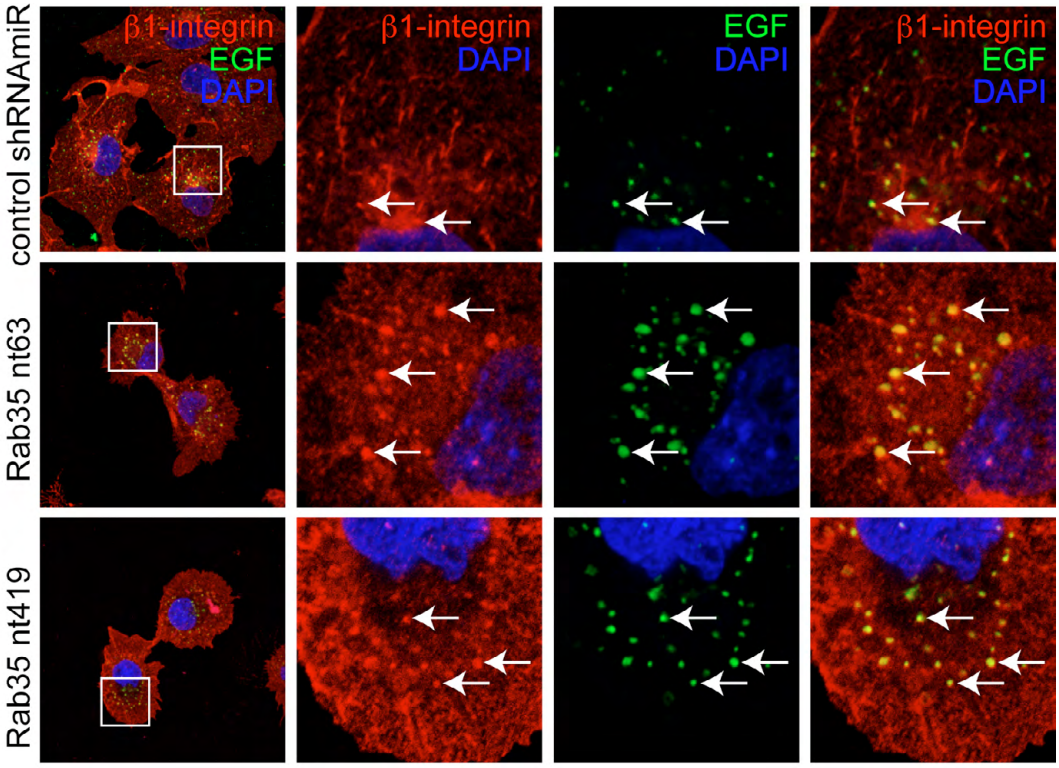

Fig. S3. β1-integrin and internalized EGF show enhanced co-localization following Rab35 knock down. COS-7 cells were treated with control shRNAmiR or two different shRNAmiRs targeting Rab35 (Rab35 nt63 and Rab35 nt419) as indicated. Cells were then serum-starved 2 h and then treated for 10 min with 2 ng/ml Alexa647-labeled EGF. Cells were then fixed and stained for endogenous β1-integrin along with DAPI to reveal the nucleus. Arrows point to enlarged intracellular vesicles containing EGF and β1-integrin.

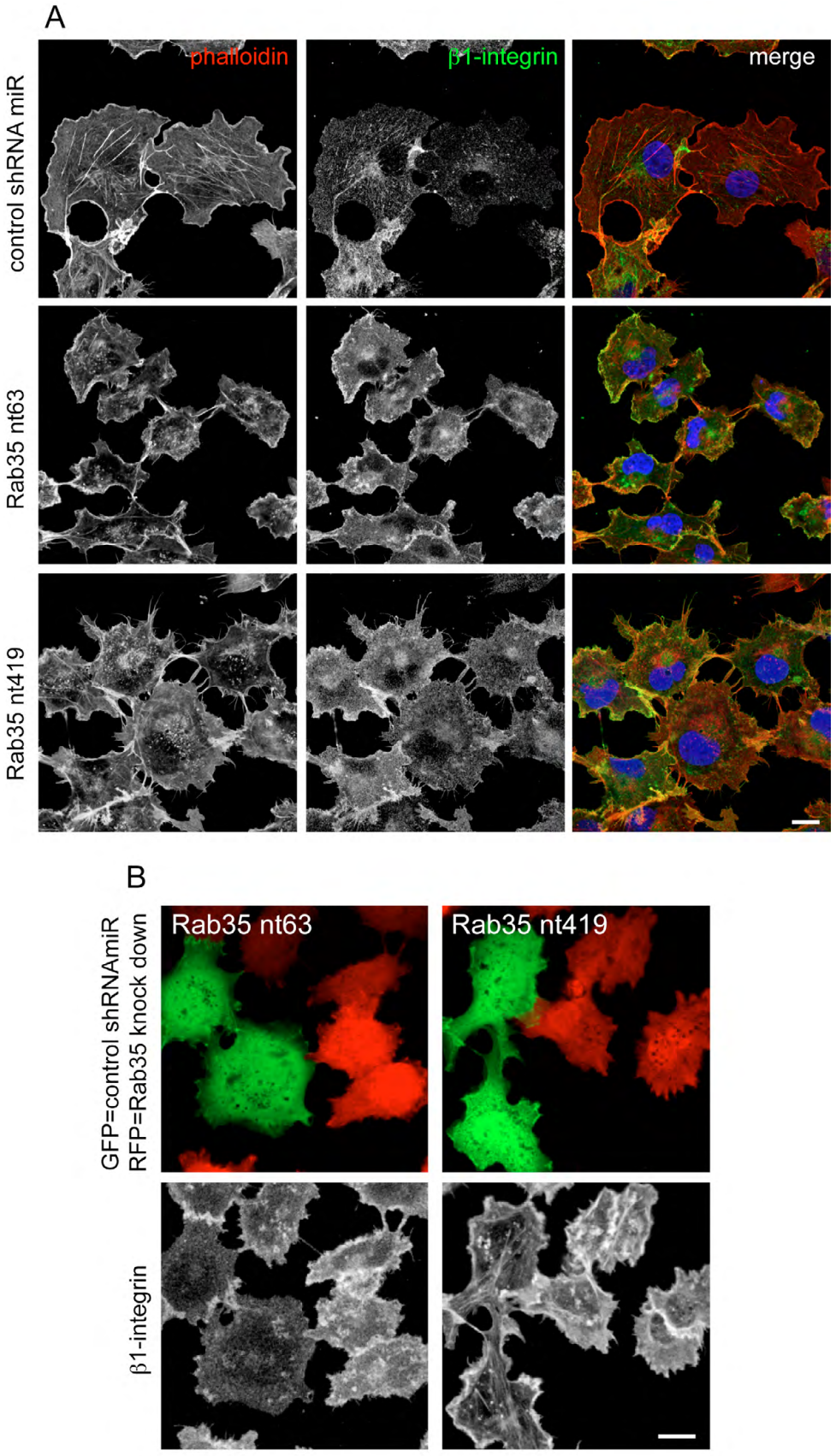

Fig. S4. Rab35 knock down cells demonstrate alterations in cell morphology. **(A)** COS-7 cells were treated with control shRNAmiR or two different shRNAmiRs targeting Rab35 (Rab35 nt63 and Rab35 nt419) as indicated. Cells were then stained with phalloidin to reveal F-actin and with an antibody recognizing β1-integrin. Scale bar = 10 μm. **(B)** COS-7 cells were treated with control shRNA driven from a plasmid also driving GFP expression or with shRNAs targeting Rab35 (Rab35 nt63 and Rab35 nt419) and driven from a plasmid also driving RFP expression. The cultures were then mixed, fixed and stained for β1-integrin. Scale bar = 10 μm.